THE INSTITUTE OF ELECTRICAL AND ELECTRONICS ENGINEERS INC.

SIGNAL PROCESSING
ALGORITHMS, ARCHITECTURES, ARRANGEMENTS, AND APPLICATIONS
SPA 2013
September 26-28th, 2013, Poznań, POLAND

# Automatic Prostate Segmentation in MR images Based on 3D Active Contours with Shape Constraints

Andrzej Skalski, Jakub Lagwa
AGH University of Science and Technology
Department of Measurement and Electronics
al. Mickiewicza 30, Kraków, Poland
skalski@agh.edu.pl

Piotr Kedzierawski
HollyCross Cancer Center
Department of Radiotherapy,
Artwińskiego 3, PL25734, Kielce, Poland
piotr.ke@op.pl

Tomasz Zielinski
AGH University of Science and Technology
Department of Telecommunications
al. Mickiewicza 30, Kraków, Poland
tzielin@agh.edu.pl

Tomasz Kuszewski
HollyCross Cancer Center
Department of Medical Physics,
Artwińskiego 3, PL25734, Kielce, Poland

*Abstract*—**Planning radiotherapy of prostate cancer requires the prostate segmentation in computed tomography (CT) images that can be manual (done by medical doctors), semi-automatic or automatic. Additional usage of magnetic resonance (MR) images, where the soft tissue are better visible, makes this operation more robust. The paper addresses the problem of prostate segmentation in MR data. Its main contribution relies on novel application of the well-known active contour (AC) method with gradient vector flow (GVF) modification to this task. It is shown in the paper that such approach is successful only after addition of a priori knowledge in the form of prostate shape constraint. The statistical prostate shape was modeled as an ellipse which parameters are calculated exploiting statistical atlas principles. It is presented using Dice similarity measure that the proposed automatic prostate segmentation offers results that are very close to the manual ones and can be used in radiotherapy planning.**

***Keywords: MRI, Magnetic Resonance, segmentation, prostate, radiotherapy, active contours, shape priors***

## I. INTRODUCTION

Radiotherapy plays a very important role in cancer treatment, especially in case of the prostate [1, 2]. Target volume to be radiated has to contain all cancer cells, obligatory rounded by a margin of healthy tissue that should be as small as possible. Typically radiation plans make use of manual organ segmentation (delineation) in the computed tomography (CT) data done by medical doctors. However in the CT data soft tissues are not clearly visible, in contrary to the magnetic resonance (MR) images. Therefore combined application of CT and MR data to soft organs (e.g. prostate) segmentation before the radiation planning was proposed and efficiency of such approach was investigated and confirmed [3, 4, 5]. At present manual segmentation is assisted by computer-aided tools offering a doctor semi-automatic and fully automatic segmentation procedures. Most of them use deformable models in the form of growing regions and active contours [6, 7]. Application of these methods to prostate segmentation in the CT images can be found in [8, 9].

The modern and efficient trend in medical data segmentation relies on creation of statistical atlases of human organs (in sense of *mean* shapes and volumes) and using them as a priori knowledge during optimization and decision taking. This knowledge is incorporated typically inside optimization processes in the form of specific constraints or additional driving forces. Atlas-like segmentation [10-12] together with Active Shape Model (ASM) or Active Appearance Model (AAM) based segmentation [13,14] represent examples of such solutions using prior information.

The present paper addresses a problem of automatic prostate segmentation not in CT, what is typical, but in MR images, additionally with usage of a priori knowledge about this organ. Several solutions of prostate segmentation in MRI have been reported in literature already: semi-automatic finding prostate boundary in polar coordinate system using scale-space ridge detection and assuming circular prostate shape [15], semi-automatic finding prostate edge using gradient flow direction and using prior knowledge of the shape of the object [16], fully-automatic fuzzy sets fusion algorithm making use of PCA-based prostate model [17], and, finally, deformable model making use of probabilistic information, including statistical prostate shape [18]. In the approach proposed now the well-known 3D active contour (AC) segmentation (snakes) method [6] with gradient vector flow (GVF) [7] is used, in similar way as for the CT data, but the procedure is additionally equipped with shape constraint (ellipsoid) resulting from statistical prostate modeling (*statistical atlas*) performed earlier by the authors in [19]. Obtained results from automatic prostate segmentation in MRIs are compared to the manual ones using Dice similarity measure [20]. They confirm correctness and efficiency of the proposed method.

The paper is organized as follows. After introduction, the research methodology is presented in section II: first, the active contour method [6] is briefly characterized, next, the prostate shape model [19] is introduced and, finally, the method of result evaluation is described [20]. Next, in section III obtained experimental results are presented and discussed. The paper ends typically with conclusions and references.

## II. METHODOLOGY

### A. Segmentation using 3D active contour

In the paper, we propose to do the prostate segmentation using 3D active contour (AC) method [6] with gradient vector flow (GVF) modification [7]. Due to known shape of a prostate being similar to an ellipsoid, a new constraint (described below) for the shape of evolving surface has been added to the AC-GVF algorithm what is the main contribution of the paper.

The active contour algorithm [6], proposed by Kass, Witkin and Terzopoulos, is a well known method in image analysis & processing, especially in computer vision. The main field of its application is data segmentation, in our case in 3D space (with voxels). The active contour model is defined as an energy-minimizing problem. Snake energy depends on its shape, image properties and location within the image. The snake is defined parametrically as:

$$\mathbf{v}(s) = [x(s), y(s), z(s)] \tag{1}$$

where $x(s)$, $y(s)$, $z(s)$ are $x$, $y$, $z$ coordinates along the contour s∈ [0, 1]. The energy functional to be minimized can be defined as [6]:

$$E_{snake} = \int_0^1 \left[ E_{\text{int}}(\mathbf{v}(s)) + E_{ext}(\mathbf{v}(s)) + E_{con}(\mathbf{v}(s)) \right] ds \tag{2}$$

where $E_{int}$ and $E_{ext}$ represent, respectively, internal and external (image) energy:

$$E_{\text{int}} = \alpha(s)\left|\frac{d\mathbf{v}(s)}{ds}\right|^2 + \beta(s)\left|\frac{d^2\mathbf{v}(s)}{ds^2}\right|^2, \tag{3a}$$

$$E_{ext} = \varpi_{line}\mathbf{I}(x,y,z) - \varpi_{edge}\left|\nabla\mathbf{I}(x,y,z)\right|^2 + \varpi_{term}E_{term}, \tag{3b}$$

α is an elasticity, β – a stiffness of snakes, $\mathbf{I}(x,y,z)$ – an image being segmented, ∇ - a gradient operator and $E_{term}$ – a curvature of contours.

The main limitation of the *snakes* approach is the requirement of snake initialization close to the final solution. Application of forces similar to balloon pumping [21]:

$$F_{ballon}(s) = \kappa\mathbf{n}(\mathbf{v}(s)) \tag{4}$$

is used as one possibility to overcome this drawback. The second solution of the problem was proposed by Xu and Prince [8] in the form of gradient vector flow (GVF) fields. In 3D the GVF is defined as a vector field $\mathbf{u}(x,y,z)$ that minimizes the following energy functional:

$$E_{GTV} = \iiint \mu\left|\nabla\mathbf{u}\right|^2 + \left|\nabla f\right|^2\left|\mathbf{u} - \nabla f\right|^2 dxdydz \tag{5}$$

where $f$ is an edge map. Details can be found in [7]. Both mentioned above techniques were used in the proposed algorithm of prostate segmentation in MR data, presented in this paper.

### B. Prostate shape constrain

In order to fit statistically the ellipsoid constraint to real data, manual prostate delineations done by medical doctors were automatically surrounded by ellipsoids (having volumes as small as possible) in CT [19] and MRI data. In order to extract the mean prostate ellipsoidal shape the Principal Component Analysis (PCA) [21] was used for the shape approximation, similarly as in [17]. The PCA choice for finding lengths of xyz-axes of approximating ellipsoid was motivated by geometrical interpretation of the PCA method [21]. In this application the PCA is not used for typical dimensionality reduction of feature space but for extraction of information concerning **principal directions** of the approximated object: their values and variations.

Ellipsoids, approximating prostates, were calculated for 22 CT and 5 MR data annotated by medical doctors. Figure 1 presents an example of 3D surface resulting from 2D manual delineations of a prostate (left) and an ellipsoid approximating it (right). For each ellipsoid a 3-element vector of features:

$$x_{ell} = [a, b, c] \tag{6}$$

was calculated, containing values of the ellipsoid half-axes. Obtained statistical results of this operation are summarized in table I.

TABLE I. SEMI-AXES OF ELLIPSOID APPROXIMATING THE PROSTATE

| **Ellipsoid approximating the prostate** | | |
|---|---|---|
| ***Axis*** | ***Mean*** | ***Std*[a]** |
| *a* | 42.33 mm | 4.77 mm |
| *b* | 37.00 mm | 3.16 mm |
| *c* | 24.10 mm | 5.72 mm |

a. Standard deviation

Calculated values were used for shape limitation of the evolving 3D active contour [6, 7] trying to segment (approximate) a prostate in the MR data. In each algorithm iteration, an ellipsoid surrounding the current contour was calculated. The strength of contour evolution was modified using lengths of the ellipsoid half-axes. However, the evolution force for each direction was modified using a correction function presented in figure 2, calculated from the model. Correction is independent for each direction. Value of the force correction coefficient (*cc*) was calculated in the following way:

$$cc_i = \begin{cases} 1 \quad \text{for} \quad d < \widetilde{d}_i - std_i \\ e^{\frac{(d-\widetilde{d}_i)^2}{2std_i^2}} \quad \text{for other cases} \end{cases} \tag{7}$$

separately for each half-axis of the ellipsoid (for $i$ equals $a$, $b$ and $c$). In (7) $\widetilde{d}_i$ and $std_i$ stand for mean and standard deviation of the separate axes – their values are given in table I.

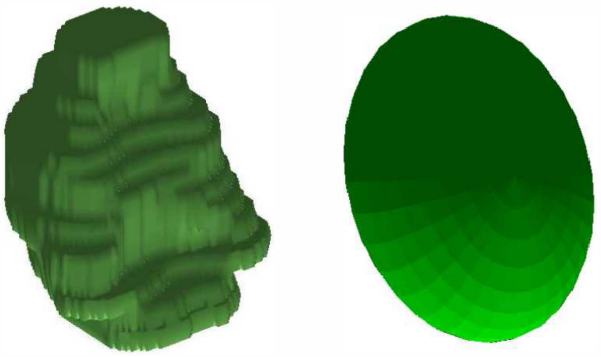

Figure 1. Example of 3D solid figure of a prostate, resulting from 2D manual delineaton of MR slices (left), and calculated ellipsoid approximating it.

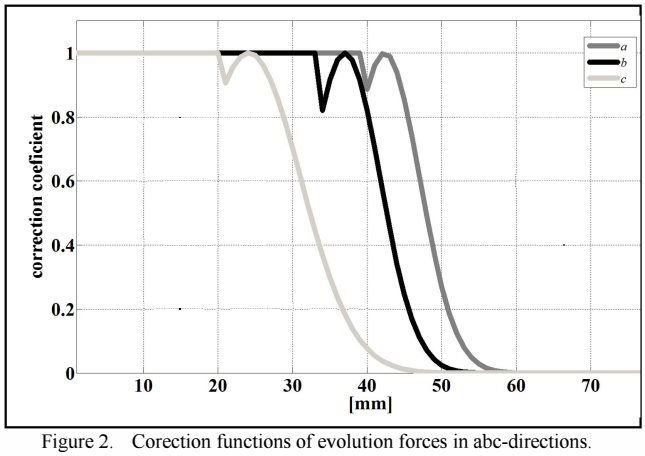


Figure 2. Corection functions of evolution forces in abc-directions.

### C. *Segmentation quality evaluation*

In order to evaluate efficiency of the proposed segmentation method, Dice similarity coefficients (DSC) [20], between regions obtained from the proposed automatic segmentation algorithm and the expert outlines, were calculated:

$$DSC\left(\mathbf{M}_A, \mathbf{M}_{GT}\right) = \frac{2\left|\mathbf{M}_A \cap \mathbf{M}_{GT}\right|}{\left|\mathbf{M}_A\right| + \left|\mathbf{M}_{GT}\right|} \qquad (7)$$

where $\mathbf{M}_A$ is a binary mask received from the algorithm and $\mathbf{M}_{GT}$ is a mask from the manual contouring by expert. This metric allows to measure the similarity of two data sets. Its range changes from 0 for disjoint sets to 1 for sets that are identical.

## III. Results

Magnetic resonance data of different patients were segmented using the method described in this work. In the computational experiments we used the available Matlab implementation of the AC+GVF algorithm [23] to which the suggested ellipsoidal prostate shape constraint was added. In all experiments the following parameter values were applied:

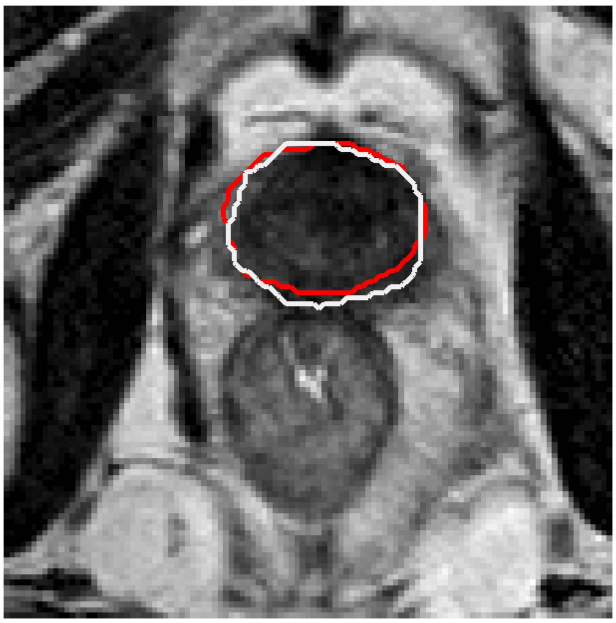

Figure 3. Example of MR slice with two segmentation results: white contour - ground truth (given manually by an expert), red contour - results from our automatic algorithm

Figure 4. Solid figures of reconstructructed prostates from MR data of different patients.

$\varpi_{line} = 1, \varpi_{edge} = 0$, smoothing shifts in $x, y, z$ direction $\delta_x = \delta_y = \delta_z = 0.5$, elasticity and stiffness $\alpha = \beta = 0.2$, weight of external force = 0.5, GVF regularization parameter $\mu = 0.1$, balloon force $\kappa = 0.2$, time step $\gamma = 0.1$ and number of iteration equal 25.

Figure 3 presents an example of the segmentation result: one slice of the MR data with two prostate delineations, the first made by an expert manually (ground truth – white line) and the second calculated by our method automatically (red/darker line).

DSC average value for 229 slices coming from 8 MR data of prostate cancer patients not included to the model was equal 0.81 with standard deviation equal 0.04 what can be interpreted as a good result.

Figure 4 presents examples of 3D prostate shapes, reconstructed from MRI of different patients. They are different despite of usage of the same statistical ellipsoidal prostate model but all of them are valid from the point of view of medical expert.

## IV. CONCLUSIONS

The new approach of prostate segmentation in magnetic resonance data was proposed in the paper. It originates from computed tomography application (active contours with gradient vector flow) but it turned out that the method works also quite well in MR case when equipped with the ellipsoidal prostate shape constraint. The method was validated by manual expert segmentation by means of Dice similarity measure. The future research will be concentrated on further optimization of the shape constraint usage during iterative segmentation procedure.

## ACKNOWLEDGMENT

The research was supported by Polish grant founded by Polish Ministry of Science and Higher Education/National Science Centre, project NN 518 497739.

## REFERENCES

[1] Cancer Research UK, Prostate Cancer - UK Incidence Statistics, http://info.cancerresearchuk.org/cancerstats/ types/prostate/incidence/.

[2] V. A. Horwich, C. Parker C., and V. Kataja, "Prostate cancer: ESMO clinical recommendations for diagnosis, treatment and follow-up," *Annals of Oncology* 20 (Supplement 4): iv76–iv78, DOI: http://annonc. oxfordjournals.org/content/20/ suppl_4/iv76.full.pdf+html.

[3] V. S. Khoo, et al., "Comparison of MRI with CT for the radiotherapy planning of prostate cancer: a feasibility study," *The British Journal of Radiology*, vol. 72, pp. 590-597, 1999.

[4] G. M Villeirs, et al,"Interobserver delineation variation using CT versus combined CT+MRI in intensity–modulated radiotherapy for prostate cancer*," Strahlentherapie und Onkologie*, no 7, pp. 424-430, 2005.

[5] G. M. Villeirs, and G. O. De Meerleer, "Magneric resonanse imagining (MRI) anatomy of the prostate and application of MRI in radiotherapy planning," *European Journal of Radiology*, vol. 63, pp. 361-368, 2007.

[6] M. Kass, A. Witkin, and D. Terzopoulos, "Snakes: active contour models*," Int. Journal of Computer Vision*, pp. 321–331, 1988.

[7] Ch. Xu, and J. L. Prince, "Snakes, shapes, and gradient vector flow," *IEEE Trans. on Image Processing*, vol. 7, no 3, pp. 359-369, 1998.

[8] M. Mazonakis, J. Damilakis, H. Varveris, P. Prassopoulos, and N. Gourtsoyiannis, "Image segmentation in treatment planning for prostate cancer using the region growing technique," *The British Journal of Radiology*, vol. 74, pp. 243-248, 2001 (CT).

[9] M. J. Costa, H. Delingette, S. Novellas, and N. Ayache, "Automatic segmentation of bladder and prostate using coupled 3D deformable models," Proc. MICCAI-2007 Conf., *LNCS* 4791 (Springer-Verlag), pp. 252-260, 2007 (CT).

[10] A. Skalski, T. Zieliński, P. Kukołowicz, P. Kędzierawski, "Computer tomography-based raditherapy planning on the example of prostate cancer: application of level-set segmentation method guided by atlas-type knowledge," *4th Int. Symp. on Applied Sciences in Biomedical and Communication Technologies ISABEL*, Barcelona, 26–29 October 2011, DOI:10.1145/2093698.2093840.

[11] O. Acosta, et al., "Atlas Based Segmentation and Mapping of Organs at Risk from Planning CT for the Development of Voxel-Wise Predictive Models of Toxicity in Prostate Radiotherapy," In: A. Madabhushi et al. (Eds.): *Prostate Cancer Imaging*, LNCS 6367, Springer-Verlag, pp. 42-51, 2010.

[12] S. Chen, M. Lovelock, R.J. Radke, "Segmenting the prostate and rectum in CT imagery using anatomical constraints," *Medical Image Analysis,* vol. 15, no. 1, pp. 1-11, Feb. 2011.

[13] A. Skalski, A. Kos, T Zieliński, "Using ASM in CT data segmentation for prostate radiotherapy," *Int Conf. on Computer Graphics and Vision* ICCVG-2012, Warsaw, Poland, LNCS 7594, pp. 610–617, September 24–26, 2012.

[14] A. Kos, T. Zielinski, A. Skalski, P. Kukolowicz, and P. Kedzierawski, "Comparison of ASM and AAM-based segmentation of prostate image in the CT scans for radiotherapy planning," *Proc. NTAV/SPA-2012 Conf.*, Łódź, pp. 53–57, September 27-29, 2012.

[15] R. Zwiggelaar,Y. Zhu, and S. Williams, "Semi-automatic segmentation of prostate," *Proc. IbPRIA-2003 Conf.*, LNCS 2652 (Springer-Verlag), pp. 1108-1116, 2003.

[16] M. Samiee, G. Thomas, and R. Fazel-Rezai, "Semi-automatic prostate segmentation of MR images based on flow orientation," *IEEE Int. Symp. on Signal Processing and Information Technology*, pp. 203-207, 2006.

[17] N. Betrouni, et al., "3D automatic segmentation and reconstruction of prostate on MR images," *Proc. IEEE EMBS Conf.*, Lyon, France, pp. 5259-5262, 2007.

[18] N. Makni, P. Puech, R. Lopes, A.S. Dewalle, O. Colot, N. Betrouni, "Combing a deformable model and a probalistic framework for an automatic 3D segmentation of prostate on MRI," *Int. Journal CARS*, no. 4, pp. 181-188, 2009.

[19] A. Skalski, J. Łągwa, P. Kędzierawski, P. Kukołowicz, "Shape analysis of abdominal structures for prostate radiotherapy process," *Measurement Automation and Monitoring*, MAaM, vol. 56, no. 4, pp. 254-257, 2013, (in Polish).

[20] K. H. Zou, et al., "Statistial validation of image segmentation quality based on a spatial overlap index," *Acad. Radiology*, vol. 11, no. 2, pp. 178-189, Feb 2004.

[21] Jolliffe I.T.: *Principal Component Analysis*. Springer-Verlag, New York, 2002.

[22] L.D. Cohen, and I. Cohen, "Finite-element methods for active contour models and balloons for 2-D and 3-D images." *IEEE Trans. on Pattern Analysis and Machine Intelligence*, vol. 15 no. 11 pp. 1131-1147, 1993.

[23] D.-J. Kroon, "Snake: Active Contour," http://www.mathworks.com/ matlabcentral/fileexchange/28149-snake-active-contour.